PHYSICAL REVIEW D **82,** 063506 (2010)

Dark matter constraints from a cosmic index of refraction

Susan Gardner[1,2,*] and David C. Latimer[2]

[1]*Center for Particle Astrophysics and Theoretical Physics Department, Fermi National Accelerator Laboratory, Batavia, Illinois 60510, USA*

[2]*Department of Physics and Astronomy, University of Kentucky, Lexington, Kentucky 40506-0055, USA*

(Received 29 January 2010; published 3 September 2010)

The dark matter candidates of particle physics invariably possess electromagnetic interactions, if only via quantum fluctuations. Taken en masse, dark matter can thus engender an index of refraction which deviates from its vacuum value. Its presence is signaled through frequency-dependent effects in the propagation and attenuation of light. We discuss theoretical constraints on the expansion of the index of refraction with frequency, the physical interpretation of the terms, and the particular observations needed to isolate its coefficients. This, with the advent of new opportunities to view gamma-ray bursts at cosmological distance scales, gives us a new probe of dark matter and a new possibility for its direct detection. As a first application we use the time delay determined from radio afterglow observations of distant gamma-ray bursts to realize a direct limit on the electric charge-to-mass ratio of dark matter of $|\varepsilon|/M < 1 \times 10^{-5}$ eV^{-1} at 95% C.L.

DOI: 10.1103/PhysRevD.82.063506 PACS numbers: 95.35.+d, 95.85.Bh, 98.70.Rz

Some 23 percent of the Universe's energy budget is in dark matter [1–3], yet, despite its abundance, little is known of its properties. A number of methods have been proposed for the detection of dark matter. Such studies typically rely, for direct searches, on dark matter-nucleus scattering, and, for indirect searches, on two-body annihilation of dark matter to standard model particles; constraints follow from the nonobservation of the aftermath of particular two-body interactions. In contrast, we probe dark matter in bulk to infer constraints on its particulate nature.

We search for dark matter by studying the modification of the properties of light upon passage through it. One can study either polarization [4] or propagation effects; we focus here on the latter. The resulting constraints are most stringent if dark matter consists of sufficiently low mass particles, be they, e.g., warm thermal relics or axion-like particles, that its number density greatly exceeds that of ordinary matter. We thus consider dark *matter*. Matter effects are signaled by dispersive effects in the speed or attenuation of light. We study this by introducing an index of refraction $n(\omega, z)$, whose deviation from unity is controlled by the light-dark matter scattering amplitude in the forward direction, i.e., the forward Compton amplitude, as well as by the angular frequency ω of the light and the redshift z at which the matter is located. A dark matter particle need not have an electric charge to scatter a photon; it need only couple to virtual electromagnetically charged particles to which the photons can couple. The scattering amplitude is related by crossing symmetry to the amplitude for dark matter annihilation into two photons, so that any dark matter model which gives rise to an indirect detection signal in the two-photon final state [5] can also drive the index of refraction of light from unity. Its real part is associated with the speed of propagation, and we search for its deviation from unity by searching for frequency-dependent time lags in the arrival of pulses from distant gamma-ray bursts (GRBs).

The limits on the nonobservation of frequency-dependent effects in the speed of light are severe. The best limits from terrestrial experiments control the variation in the speed of light c with frequency to $|\delta c|/c \lesssim 1 \times 10^{-8}$ [6], but the astrophysical limits are much stronger. The arrival time difference of pulses from the Crab nebula bound $|\delta c|/c \lesssim 5 \times 10^{-17}$ [7,8], and still better limits come from the study of GRBs [8,9]. GRBs are bright, violent bursts of high-energy photons lasting on the order of thousandths to hundreds of seconds, and their brightness makes them visible at cosmological distances. Time delays which are linear in the photon energy can occur *in vacuo* in theories of quantum gravity; the special features of GRBs make them particularly well suited to searches for such signatures of Lorentz violation [9]. The detection of photons of up to ~31 GeV in energy from GRB 090510 severely constrains this scenario, placing a lower limit on the energy scale at which such linear energy dependence occurs to 1.2 $E_{\rm Planck} \approx 1.5 \times 10^{19}$ GeV [10]. Although vacuum Lorentz violation and light-dark matter interactions can each induce dispersive effects, their differing red shift and frequency dependence render them distinct.

A model-independent analysis of the deviation of the refractive index from unity is possible if we assume that the photon energy is small compared to the energy threshold required to materialize the electromagnetically charged particles to which the dark matter can couple. In models of electroweak-symmetry breaking which address the hier-

*Permanent Address Department of Physics and Astronomy, University of Kentucky, Lexington, KY 40506-0055, USA.

archy problem, a dark matter candidate can emerge as a by-product. In such models the inelastic threshold $\omega_{\rm th}$ is commensurate with the weak scale, or crudely with energies in excess of $\mathcal{O}(200\ {\rm GeV})$, as the new particles are produced in pairs. If the photon energy ω satisfies the condition $\omega \ll \omega_{\rm th}$, we can apply the techniques of low-energy physics to the analysis of the forward Compton amplitude. Under an assumption of Lorentz invariance and other symmetries, we expand the forward Compton amplitude in powers of ω and give a physical interpretation to the coefficients of the first few terms as $\omega \to 0$ [11–13]. In particular, the term in $\mathcal{O}(\omega^0)$ is controlled by the dark matter particles' charge and mass, weighted by preponderance, irrespective of all other considerations save our assumption of Lorentz invariance [14].

The relationship between the index of refraction $n(\omega)$ and the forward scattering amplitude $f_\omega(0)$ for the light of angular frequency ω is well known [15,16], where we relate $f_\omega(0)$ to the matrix element $\mathcal{M}$ of quantum field theory to connect to particle physics models of dark matter. Using standard conventions [17], we determine $n(\omega) = 1 + (\rho/4M^2\omega^2)\mathcal{M}_r(k,\, p \to k,\, p)$, in the matter rest frame [15], so that $p = (M, \mathbf{0})$ and $k = (\omega, \omega\hat{\mathbf{n}})$ with ρ, the mass density of the scatterers and M, the particle mass. In our analysis we assume $M \gg T(z)$, where $T(z)$ is the temperature of the dark matter at the red shift of the observed gamma-ray burst. Since $T(z)$ should be a factor of some $((1+z)/(1+z_{\rm prod}))^{1-2}$ smaller than $T(z_{\rm prod})$ at the moment of its production or decoupling, our limits are not restricted to cold dark matter exclusively. Moreover, even in the latter case, the candidate mass can be as light, e.g., as light as $M \sim 6 \times 10^{-6}$ eV in the axion model with Bose-Einstein condensation of Ref. [18]. Under the assumptions of causality or, more strictly, of Lorentz invariance, as well as of charge-conjugation, parity, and time-reversal symmetry in the photon-dark matter interaction, we have [11,13] $\mathcal{M}_r(k,\, p \to k,\, p) = f_1(\omega)\boldsymbol{\epsilon}'^{*}\cdot\boldsymbol{\epsilon} + i f_2(\omega)\mathcal{S}\cdot\boldsymbol{\epsilon}'^{*}\times\boldsymbol{\epsilon}$, where $\mathcal{S}$ is the spin operator associated with the dark matter particle and $\boldsymbol{\epsilon}$ ($\boldsymbol{\epsilon}'$) is the polarization vector associated with the photon in its initial (final) state. The functions $f_1(\omega)$ and $f_2(\omega)$ are fixed in terms of the dark matter electric charge and magnetic moment, respectively, as $\omega \to 0$ [14,19,20] without further assumption—it does not even matter if the dark matter particle is composite. The amplitude $\mathcal{M}_r(k,\, p \to k,\, p)$ is implicitly a 2×2 matrix in the photon polarization, and its diagonal matrix elements describe dispersion in propagation and attenuation [16]. The $f_2(\omega)$ term describes changes in polarization with propagation, so that we need not consider it further. Under analyticity and unitarity, expanding $f_1(\omega)$ for $\omega \ll \omega_{\rm th}$ yields a series in positive powers of ω^2 for which the coefficient of every term of $\mathcal{O}(\omega^2)$ and higher is positive definite [11,12]. Thus, a term in $n(\omega)$ which is linear in ω, discussed as a signature of Lorentz violation [9,21], does not appear if $\omega < \omega_{\rm th}$ and the medium is unpolarized. We parametrize the forward Compton amplitude as $\mathcal{M}_r = \sum_{j=0} A_{2j}\omega^{2j}$, where $A_0 = -2\varepsilon^2 e^2$ [14,17] and the dark matter millicharge is εe. The terms in $\mathcal{O}(\omega^2)$ and higher are associated with the polarizabilities of the dark-matter candidate.

Dispersive effects in light propagation are controlled by the group velocity v_g, so that the light emitted from a source a distance l away has an arrival time of $t(\omega) = l/v_g$. For very distant sources we must also take the cosmological expansion into account [22], so that as we look back to a light source at redshift z, we note that the dark matter density accrues a scale factor of $(1+z)^3$, whereas the photon energy is blue shifted by a factor of $1+z$ relative to its present-day value ω_0 [22]. Thus, the light arrival time $t(\omega_0, z)$ is

$$t(\omega_0, z) = \int_0^z \frac{dz'}{H(z')}\left(1 + \frac{\rho_0(1+z')^3}{4M^2}\left(\frac{-A_0}{((1+z')\omega_0)^2} + A_2 + 3A_4(1+z')^2\omega_0^2 + \mathcal{O}(\omega_0^4)\right)\right), \quad (1)$$

with the Hubble rate $H(z') = H_0\sqrt{(1+z')^3\Omega_M + \Omega_\Lambda}$. We employ the cosmological parameters determined through the combined analysis of WMAP 5 yr data in the ΛCDM model with distance measurements from Type Ia supernovae (SN) and with baryon acoustic oscillation information from the distribution of galaxies [3]. Thus the Hubble constant today is $H_0 = 70.5 \pm 1.3\ {\rm km\,s^{-1}\,Mpc^{-1}}$, whereas the fraction of the energy density in matter relative to the critical density today is $\Omega_M = 0.274 \pm 0.015$ and the corresponding fraction of the energy density in the cosmological constant Λ is $\Omega_\Lambda = 0.726 \pm 0.015$ [3].

We find that the time delay is characterized by powers of ω^2 and unknown coefficients A_{2j}. Different strategies must be employed to determine them. The A_2 term incurs no frequency-dependent shift in the speed of light, so that to infer its presence one needs a distance measure independent of z, much as in the manner one infers a nonzero cosmological constant from Type Ia supernovae data. Interestingly, as $A_2 > 0$ it has the same phenomenological effect as a nonzero cosmological constant; the longer arrival time leads to an inferred larger distance scale. Cosmologically, though, its effect is very different as it scales with the dark-matter density; it acts as grey dust. The remaining terms can be constrained by comparing arrival times for differing observed ω_0.

The determination of A_0 and A_4 require the analysis of the GRB light curves at extremely low and high energies, respectively, and probe disjoint dark matter models. As a first application of our method, we use radio afterglow data to determine A_0 and thus to yield a direct limit on the electric charge to mass of dark matter. This quantity gives insight into the mechanism of dark matter stability. If dark matter possesses an internal symmetry, e.g., it cannot decay to lighter particles and conserve its hidden charge.

Such dynamics can also conspire to give dark matter a slight electric charge [23–25], which, no matter how small, reveals the existence of its hidden interactions and the reason for its stability.

To determine A_0 we consider GRBs with known redshift in which a radio afterglow is also detected. We collect the data and describe the criteria used in its selection in the supplementary material [26]. The time lag between the initial detection of the GRB at some energy and the detection of the radio afterglow is $\tau = t(\omega_0^{\rm low}, z) - t(\omega_0^{\rm high}, z)$. If we first observe the GRB at keV energies and compare with the observed arrival time in radio frequencies, then the terms in positive powers of ω_0, as well as the term in $1/(\omega_0^{\rm high})^2$, are negligible; we let $\omega \equiv \omega_0^{\rm low}$. In order to assess reliable limits on A_0 we must separate propagation effects from intrinsic source effects. Statistically, we expect time delays intrinsic to the source to be independent of z, and the time delay from propagation to depend on z and ω in a definite way. Such notions have been previously employed in searches for Lorentz invariance violation [21]. We separate propagation and emission effects, respectively, via

$$\frac{\tau}{1+z} = \tilde{A}_0 \frac{K(z)}{\nu^2} + \delta((1+z)\nu), \qquad (2)$$

where $K(z) \equiv (1+z)^{-1} \int_0^z dz(1+z')H(z')^{-1}$ depends on the cosmological past through the Hubble rate $H(z)$ and $\delta((1+z)\nu)$ allows for a frequency-dependent time lag for emission from the GRB in the GRB rest frame. The frequency $\nu \equiv \omega/2\pi$, and $\tilde{A}_0$ contains the millicharge-to-mass ratio ε/M, i.e., $4\pi^2\tilde{A}_0 = -A_0\rho_0/4M^2 = 2\pi\alpha\varepsilon^2\rho_0/M^2$ with $\rho_0 \simeq 1.19 \times 10^{-6}$ GeV/cm^3 [3] and α, the fine-structure constant. To provide a context, we first consider the value of $|\varepsilon|/M$ which would result were we to attribute the time lag associated with the radio afterglow of one GRB to a propagation effect. Choosing the GRB with the largest value of $K(z)/\nu^2$, we have a time lag of a 2.700 ± 0.006 day associated with GRB 980703A at $z = 0.967 \pm 0.001$ measured at a frequency of 1.43 GHz. With Eq. (2), setting $\delta = 0$, and noting that $K(z)/\nu^2 = 1170 \pm 10$ Mpc GHz^{-2} if the errors in its inputs are uncorrelated, the measured time lag fixes $|\varepsilon|/M \simeq 9 \times 10^{-6}$ eV^{-1}. Since there are no known examples of a radio afterglow preceding a GRB, this single time lag in itself represents a conservative limit. Turning to our data sample of 53 GRBs, we plot the measured time lag versus $K(z)/\nu^2$ in Fig. 1 and make a least-squares fit of Eq. (2) to determine $\tilde{A}_0$ and $\delta((1+z)\nu)$. We require $\tilde{A}_0 > 0$ as demanded by our model. Fitting to the points with frequencies of 4.0–75 GHz in the GRB rest frame, we determine $|\varepsilon|/M < 1 \times 10^{-5}$ eV^{-1} at 95% CL, which is comparable to our limit derived from a single observation of GRB 980703A. The dependence of our fit results on the selected frequency window, as well as the stability of our fits to the significance of the radio afterglow observation, to evolution effects in z, and to the more poorly determined red shifts and radio afterglows is discussed in the supplementary information [26].

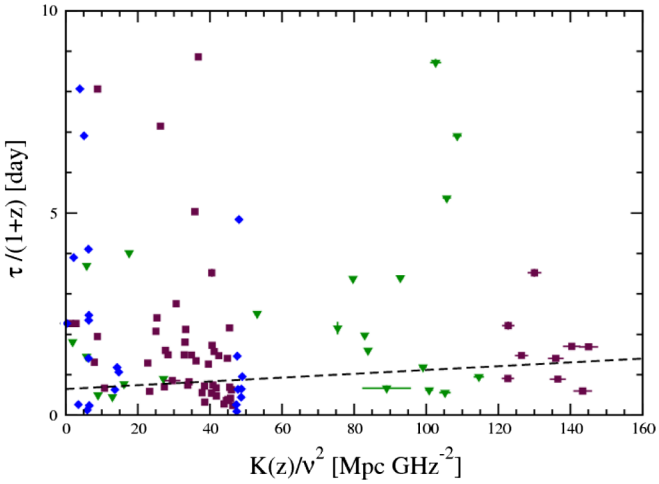

FIG. 1 (color online). The time lag τ determined from the observation of a GRB and its radio afterglow plotted as a function of $K(z)/\nu^2$ with $\nu = \omega/2\pi$, employing the data reported in the supplementary material [26]. The points correspond to frequency windows of 4.0–12 GHz (green triangles), 12–30 GHz (maroon squares), and 30–75 GHz (blue diamonds) in the GRB rest frame. Points with $(1+z)\nu < 4.0$ GHz do not appear within the chosen frame of the figure. The fit of Eq. (2) to the data with $(1+z)\nu > 4.0$ GHz with a scale factor in the uncertainty in $\tau/(1+z)$ of 450, to compensate for environmental effects in the vicinity of the emission from the GRB, yields $\tilde{A}_0 = 0.0010 \pm 0.0019$ day Ghz^2 Mpc^{-1} and $\delta = 0.65 \pm 0.10$ day with $\chi^2/\text{ndf} = 1.13$. Thus, $\tilde{A}_0 < 0.005$ day Ghz^2 Mpc^{-1} at 95% C.L. to yield $|\varepsilon|/M < 1 \times 10^{-5}$ eV^{-1} at 95% C.L. The statistical scale factors are not shown explicitly. For clarity of presentation we display time lags in the GRB rest frame of less than 10 days only.

We have found a direct observational limit on the dark matter electric charge-to-mass ratio. Our study probes for a charge imbalance averaged over cosmological distance scales, without regard to its sign, at distance scales shorter than the wavelengths of the radio observations in our data set. Our bound rules out the possibility of charged "Q-balls" [25,27] of less than 100 keV in mass as dark matter candidates. Our limit holds regardless of the manner in which the dark matter is produced, though we can compare it to limits arising from the nonobservation of the effects of millicharged particle production. For example, for $M \sim 0.05$ eV, they are crudely comparable to the strongest bound from laboratory experiments [28,29], for $|\varepsilon| < 3$–4×10^{-7} for $M \lesssim 0.05$ eV [29]. In comparison the model-independent bound arising from induced distortions in the cosmic microwave background (CMB) radiation is $|\varepsilon| \leq 10^{-7}$ for $M < 0.1$ eV, though model-dependent constraints reach $|\varepsilon| \leq 10^{-9}$ for $M < 2 \times 10^{-4}$ eV [30]. Cosmological limits also arise from observations of the Sunyaev-Zeldovich effect for which, e.g., $|\varepsilon| \leq 3 \times 10^{-7}$

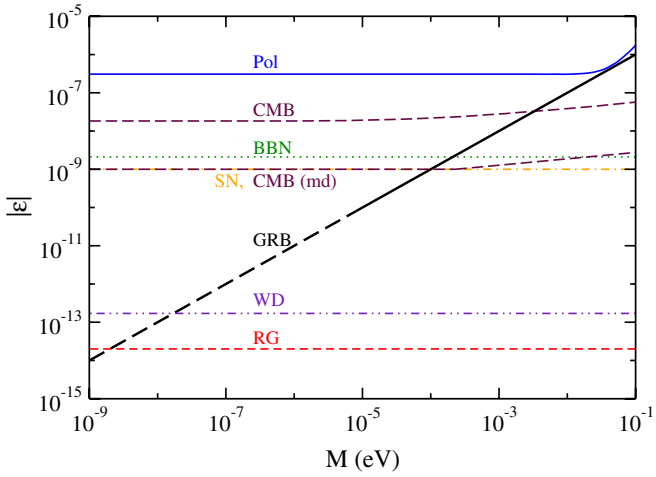

FIG. 2 (color online). Comparison of our direct limit on the absolute electric charge of dark matter, $|\varepsilon|$, in units of e with candidate mass M with limits from other sources stemming from millicharged particle production. Our limit derives from observations of GRBs and their radio afterglows and is marked "GRB" (solid black line), so that the region above that line is excluded. The condition $\omega < \omega_{\rm th}$, as discussed in the text, sets the lower endpoint of the solid line. Since Eq. (2) persists in QED, for which $\omega_{\rm th} = 0$, we expect our limit to persist for lighter, cold dark matter as well, as indicated by the dashed line. The strongest laboratory limits, which are for fermions, are marked "Pol" (solid blue line) [29], and the strongest limits from induced distortions in the CMB, which are also for fermions, are marked "CMB" (long-dashed maroon line)—the upper curve is the model-independent limit, whereas the lower curve is the model-dependent (md) limit [30]. Constraints on $|\varepsilon|$ emerge from limits on novel energy-loss mechanisms in stars and supernovae; such limits also fail to act if $|\varepsilon|$ is too large. The limit from plasmon decay in red giants is marked by "RG" (short-dashed red line) [28], the same limit in white dwarfs is marked by "WD" (dot-dot-dashed indigo line) [28], and the limit from SN 1987A is marked by "SN" (dot-dashed orange line) [28]. The RG limit acts if $|\varepsilon| \lesssim 10^{-8}$ [28]. We have also reported the limit from big-bang nucleosynthesis, marked by "BBN" (dotted green line), from Ref. [28] as well.

for $M \sim 10^{-6}$ eV [31]. For these light masses our limit is stronger, which shows that millicharged particles of such mass and charge are not the primary constituents of dark matter. Limits also arise from stellar evolution and big-bang nucleosynthesis constraints, for which the strongest is $|\varepsilon| < 2 \times 10^{-14}$ for $M < 5$ keV [28], as well as from the manner in which numerical simulations of galactic structure confront observations [32–34]. We offer a visual summary of this discussion in Fig. 2. Indirect limits can be evaded, for example, in some models, the dynamics which gives rise to millicharged matter are not operative at stellar temperatures [29,35]; other models evade the galactic structure constraints [25,27].

Our limit also significantly restricts the phase space of models with hyperweak gauge interactions and millicharged particles which can arise in string theory scenarios [31,36] as viable dark matter candidates. We estimate that our limit can be improved considerably before the dispersive effects from ordinary charged matter become appreciable [37]. The largest such contribution to $\tilde{A}_0$ should come from free electrons. We estimate the cosmological free electron energy density ρ_e to be no larger than $\rho_e = (M_e/M_p)\rho_{\rm cr}\Omega_b \approx 0.130\ {\rm eV/cm^3}$ [3], where Ω_b is the fraction of the energy density in baryons with respect to the critical density today and M_e and M_p are the electron and proton mass, respectively. Replacing ρ_0 with ρ_e and ε/M with $1/M_e$ in $\tilde{A}_0$ we find that our limit would have to improve by $\mathcal{O}(2 \times 10^{-3})$ before the contribution from free electrons could be apparent. We set our limit of $|\varepsilon|/M < 1 \times 10^{-5}\ {\rm eV}^{-1}$ from existing radio observations at no less than 4 GHz in the GRB rest frame, so that our limit is certainly operative if $\omega_{\rm th}/2\pi > 4$ GHz, or crudely, if $M > 8 \times 10^{-6}$ eV. Studies of the polarizability in QED [38], for which $\omega_{\rm th} = 0$, also reveal the analytic structure in ω we have assumed for the forward Compton amplitude. Thus, we believe our limit to be of broader validity, so that the lower limit on the mass can be less than 8×10^{-6} eV, though it is model dependent and set by the Lee-Weinberg constraint [39], much as the minimum mass of $\sim 6 \times 10^{-6}$ eV is determined in the axion model of Ref. [18]. Forward scattering is coherent irrespective of whether the photon wavelength is large compared to the interparticle spacing, so that we expect our results to persist in the dilute particle limit as well, as supported by laboratory studies [40]. One further comment: at a frequency of 4 GHz our limit implies that we probe the average net charge of dark matter, with no constraint on its sign, at length scales of no longer than 8 cm. Our limits can be significantly bettered through GRB radio afterglow studies at longer wavelengths.

We thank Keith Olive for an inspiring question and Scott Dodelson, Renée Fatemi, Wolfgang Korsch, and Tom Troland for helpful comments. S. G. would also like to thank Stan Brodsky for imparting an appreciation of the low-energy theorems in Compton scattering and the Institute for Nuclear Theory and the Center for Particle Astrophysics and Theoretical Physics at Fermilab for their gracious hospitality. This work is supported, in part, by the U.S. Department of Energy under Contract No. DE-FG02-96ER40989.

[1] D. N. Spergel *et al.* (WMAP Collaboration), Astrophys. J. Suppl. Ser. **148**, 175 (2003).
[2] M. Tegmark *et al.* (SDSS Collaboration), Phys. Rev. D **69**, 103501 (2004).
[3] E. Komatsu *et al.* (WMAP Collaboration), Astrophys. J. Suppl. Ser. **180**, 330 (2009).
[4] S. Gardner, Phys. Rev. Lett. **100**, 041303 (2008).
[5] P. Ullio, L. Bergstrom, J. Edsjo, and C. G. Lacey, Phys. Rev. D **66**, 123502 (2002).
[6] J. L. Hall, in *Atomic Masses and Fundamental Constants*, edited by J. H. Sanders and A. H. Wapstra (Plenum, New York, 1976), p. 322.
[7] B. Warner and R. Nather, Nature (London) **222**, 157 (1969).
[8] B. E. Schaefer, Phys. Rev. Lett. **82**, 4964 (1999).
[9] G. Amelino-Camelia *et al.*, Nature (London) **393**, 763 (1998).
[10] A. A. Abdo *et al.* (Fermi LAT Collaboration), Nature (London) **462**, 331 (2009).
[11] M. Gell-Mann, M. L. Goldberger, and W. E. Thirring, Phys. Rev. **95**, 1612 (1954).
[12] M. L. Goldberger, Phys. Rev. **97**, 508 (1955).
[13] T. R. Hemmert, B. R. Holstein, J. Kambor, and G. Knöchlein, Phys. Rev. D **57**, 5746 (1998).
[14] W. E. Thirring, Philos. Mag. **41**, 1193 (1950).
[15] E. Fermi, *Nuclear Physics* (University of Chicago Press, Chicago, 1974), p. 202.
[16] R. G. Newton, *Scattering Theory of Waves and Particles* (McGraw-Hill, New York, 1966), p. 24ff.
[17] M. E. Peskin and D. V. Schroeder, *An Introduction to Quantum Field Theory* (Addison-Wesley Publishing Company, Reading, MA, 1995).
[18] P. Sikivie and Q. Yang, Phys. Rev. Lett. **103**, 111301 (2009).
[19] L. I. Lapidus and Chou Kuang-Chao, Zh. Eksp. Teor. Fiz. **39**, 1286 (1960); Sov. Phys. JETP **12**, 898 (1961).
[20] S. J. Brodsky and J. R. Primack, Ann. Phys. (N.Y.) **52**, 315 (1969).
[21] J. R. Ellis *et al.*, Astrophys. J. **535**, 139 (2000).
[22] U. Jacob and T. Piran, J. Cosmol. Astropart. Phys. 01 (2008) 031.
[23] B. Holdom, Phys. Lett. **166B**, 196 (1986).
[24] D. Feldman, Z. Liu, and P. Nath, Phys. Rev. D **75**, 115001 (2007).
[25] A. Kusenko and P. J. Steinhardt, Phys. Rev. Lett. **87**, 141301 (2001).
[26] See supplementary material at http://link.aps.org/supplemental/10.1103/PhysRevD.82.063506.
[27] I. M. Shoemaker and A. Kusenko, Phys. Rev. D **78**, 075014 (2008).
[28] S. Davidson, S. Hannestad, and G. Raffelt, J. High Energy Phys. 05 (2000) 003.
[29] M. Ahlers *et al.*, Phys. Rev. D **77**, 095001 (2008).
[30] A. Melchiorri, A. Polosa, and A. Strumia, Phys. Lett. B **650**, 416 (2007).
[31] C. Burrage, J. Jaeckel, J. Redondo, and A. Ringwald, J. Cosmol. Astropart. Phys. 11 (2009) 002.
[32] B. A. Gradwohl and J. A. Frieman, Astrophys. J. **398**, 407 (1992).
[33] L. Ackerman, M. R. Buckley, S. M. Carroll, and M. Kamionkowski, Phys. Rev. D **79**, 023519 (2009).
[34] J. L. Feng, M. Kaplinghat, H. Tu, and H. B. Yu, J. Cosmol. Astropart. Phys. 07 (2009) 004.
[35] E. Massó and J. Redondo, Phys. Rev. Lett. **97**, 151802 (2006).
[36] C. P. Burgess *et al.*, J. High Energy Phys. 07 (2008) 073.
[37] L. Bombelli and O. Winkler, Classical Quantum Gravity **21**, L89 (2004).
[38] E. Llanta and R. Tarrach, Phys. Lett. **78B**, 586 (1978).
[39] B. W. Lee and S. Weinberg, Phys. Rev. Lett. **39**, 165 (1977).
[40] G. K. Campbell *et al.*, Phys. Rev. Lett. **94**, 170403 (2005).